

Graphene–Graphene Interactions: Friction, Superlubricity, and Exfoliation

Robert C. Sinclair, James L. Suter, and Peter V. Coveney*

Graphite's lubricating properties due to the "weak" interactions between individual layers have long been known. However, these interactions are not weak enough to allow graphite to readily exfoliate into graphene on a large scale. Separating graphite layers down to a single sheet is an intense area of research as scientists attempt to utilize graphene's superlative properties. The exfoliation and processing of layered materials is governed by the friction between layers. Friction on the macroscale can be intuitively understood, but there is little understanding of the mechanisms involved in nanolayered materials. Using molecular dynamics and a new forcefield, graphene's unusual behavior in a superlubric state is examined, and the energy dissipated between two such surfaces sliding past each other is shown. The dependence of friction on temperature and surface roughness is described, and agreement with experiment is reported. The accuracy of the simulated behavior enables the processes that drive exfoliation of graphite into individual graphene sheets to be described. Taking into account the friction between layers, a peeling mechanism of exfoliation is predicted to be of lower energy cost than shearing.

In the remarkable study of Feng et al.,^[1] a scanning tunneling microscope (STM) tip was used to push graphene flakes over a graphitic substrate to examine the frictional behavior of graphene nanoflakes. The flake was initially in an AB stacking orientation, the lowest energy configuration for graphite layers (see Figure 1c). The authors found that once the graphene flake was pushed out of this preferred arrangement, the superlubric nature of graphene caused the flakes to "slip" large distances of many times their diameter after they had been dislodged, before becoming "stuck" in another commensurate position. They found that the flakes on average travel further at lower temperatures, which they attributed to the reduced thermal fluctuations in the substrate.

Using classical molecular dynamics simulations with a new forcefield called GraFF (see the Computational Methods), we recreated this experimental setup. GraFF employs an angular

nonbonded potential developed using data from experiments and quantum calculations.^[2–5] The GraFF forcefield recreates the energy barrier for graphene sheets sliding past each other,^[6] allowing us to accurately simulate the behavior of superlubric^[7] graphene including the motion of the graphene flakes^[8] (for more details, see Section I in the Supporting Information).

Flakes 10 nm in diameter were chosen, which is within the range of flakes used experimentally by Feng et al.^[1] Propulsion by an STM tip was simulated by applying a constant force to each atom in the flake until it had been displaced from its commensurate position. Due to the inherently chaotic nature of the motion of the graphene flake over the substrate, a large number of simulations (40) were performed, from which we analyzed the average distance traveled by the flake. Our

simulations, for the first time, recreate the trend observed by Feng et al.: the straight-line distance traveled by the graphene flake is much further at lower temperatures. This is the case whether the substrate is graphite (modeled as four-layer graphene) or a suspended single graphene sheet (see Table 1). It should be noted that standard forcefields that only use simple Lennard–Jones nonbonded interactions^[9,10] cannot reproduce these effects. Our simulations show that using these forcefields the flakes slip after propulsion and slide for as long as we simulated them (after 10 ns the flakes had traveled over 1000 nm, already an order of magnitude greater than that seen in experiments), therefore fatally underestimating the friction.

The motion of a graphene flake propelled over a graphitic substrate is characterized by fleeting alignments with the underlying lattice during which the flake is scattered and energy is converted between translational and rotational energy. These alignment events are how friction is manifested on the nanoscale as energy is also dissipated to the bulk during each event (see Figure 1b; the alignment events are indicated by the dotted vertical lines), causing the flake to slow down and energy to be transferred to the substrate. When in an incommensurate position, the flake sees an almost uniform potential energy surface (PES) in the lateral plane,^[11] as shown by the flat interaction energy between the flake and the substrate in Figure 1b. The flake therefore slides and rotates unimpeded, a phenomenon known as superlubricity. Whenever the flake's orientation is an integer multiple of 60°—due to the hexagonal symmetry of graphene—there is a fluctuation in the interaction

R. C. Sinclair, Dr. J. L. Suter, Prof. P. V. Coveney
Centre for Computational Sciences – University College London
20 Gordon Street, London WC1H 0AJ, UK
E-mail: p.v.coveney@ucl.ac.uk

 The ORCID identification number(s) for the author(s) of this article can be found under <https://doi.org/10.1002/adma.201705791>.

© 2018 The Authors. Published by WILEY-VCH Verlag GmbH & Co. KGaA, Weinheim. This is an open access article under the terms of the Creative Commons Attribution License, which permits use, distribution and reproduction in any medium, provided the original work is properly cited.

DOI: 10.1002/adma.201705791

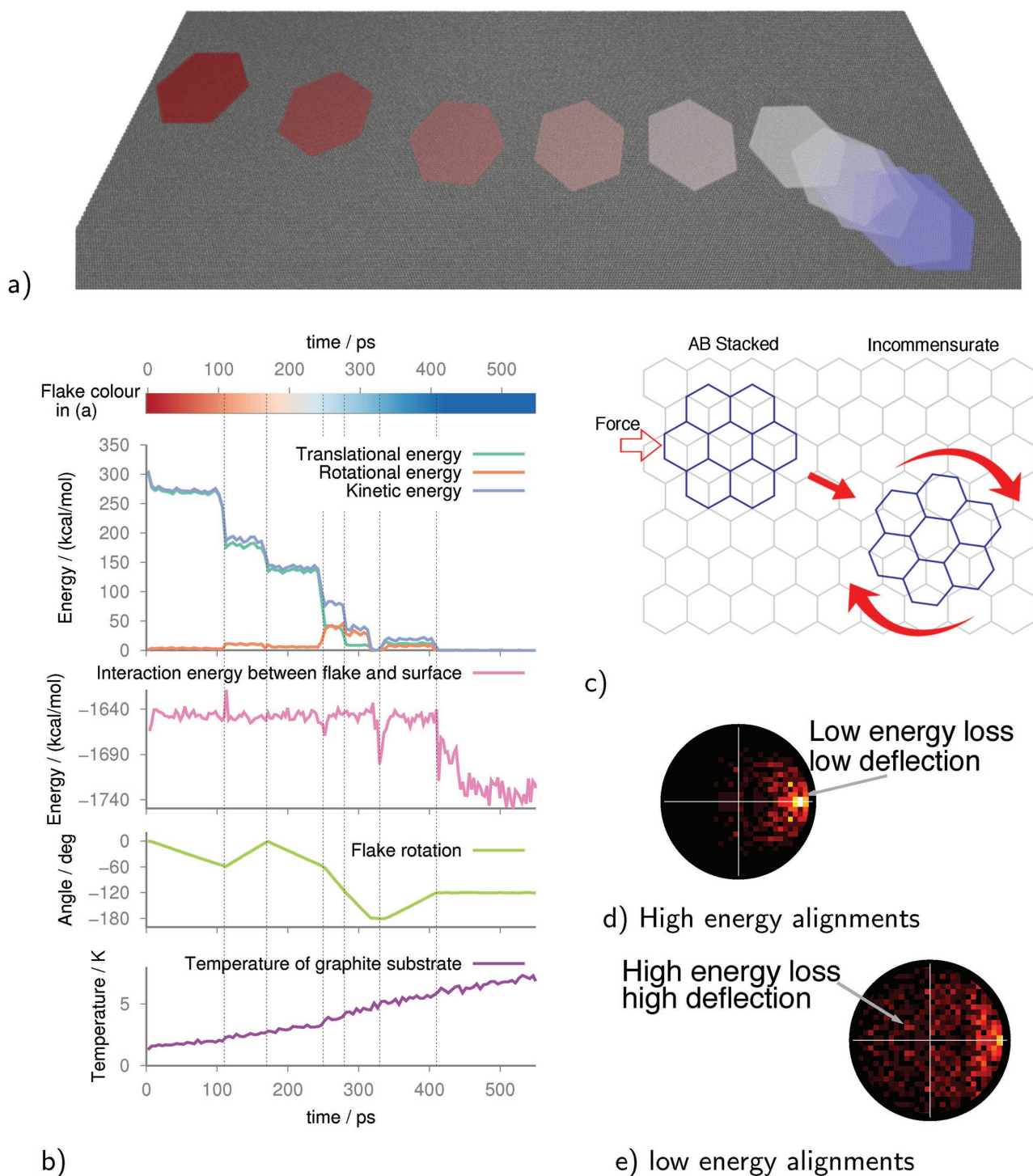


Figure 1. a) A representative trajectory from a large ensemble of simulations of a 10 nm graphene flake on a graphite surface after being pushed out of a commensurate position. In this instance, the trajectory lasted 500 ps until the flake was stationary. The flake travels from left to right, with color corresponding to time (red at the start, blue at the end). A snapshot of the flake is shown every 50 ps. The flake slides and rotates freely when unaligned with the surface lattice and is only deflected when it is aligned. The internal kinetic energy of the flake is shown in (b). The flake loses energy which is dissipated to the substrate in alignment events which are represented by dashed vertical lines in (b), until it comes to rest in a commensurate position. c) Schematic of the simulation setup. The flake, in blue, is pushed with a continuous force until it has been dislodged from its commensurate AB stacked configuration. Once free it is able to slide and rotate, essentially frictionlessly. The angle of deflection and energy lost in each alignment event are compiled into histograms in panels (d) and (e). Alignment events are shown when the kinetic energy of the flake is above 100 kcal mol⁻¹ (d) and below 100 kcal mol⁻¹ (e).

Table 1. Average straight-line distances traveled by a graphene flake on a graphitic substrate after being dislodged from a commensurate position. The flakes used in the experiment by Feng et al.^[1] ranged from 8 to 18 nm while in our simulations we used 10 nm flakes. Surface roughness, caused by increasing the temperature or reducing the substrate's rigidity, increases friction. Simulations use periodic boundary conditions. Errors are calculated from a bootstrap of 40 replicas explained in the Experimental Section; errors were not reported for the experiment.

Experiment		
Temperature [K]	Distance [nm]	
5	95	
77	35	
Simulation		
Temperature [K]	Graphite substrate distance [nm]	Suspended graphene substrate distance [nm]
1	68.8 (+12.8/−10.8)	47.9 (+5.0/−4.5)
100	35.4 (+4.1/−3.7)	29.3 (+5.2/−4.4)
200	44.7 (+6.8/−5.9)	25.9 (+2.8/−2.5)

energy between flake and surface; this is because, in the narrow window when the flake is aligned, the PES has a defined well. This results in a deflection of the center of mass trajectory, and exchange of translational and rotational energy.

When the flake has a low enough energy the wells in the PES can trap the flake. The difference in the nonbonded energy between the flake and surface for commensurate and incommensurate arrangements is ≈ 100 kcal mol^{−1}. When the internal kinetic energy of the flake (the blue line in Figure 1b) is above 100 kcal mol^{−1}, deflection after alignment events tends to be small; below, larger deflections are more probable as the flake moves more slowly until it encounters a commensurate position in which to settle. This is shown in Figure 1d, where we plot the distribution of kinetic energies and deflections of a flake after alignment events, the radial distance being given by $E_{\text{incident}}/E_{\text{deflected}}$, and the angle from the x -axis is the deviation of the center of mass trajectory, i.e., a point on the circumference of Figure 1d would have lost no kinetic energy after aligning with the substrate lattice and a point on the left of the y -axis would have been deflected by greater than 90°.

An illustrative trajectory is shown in Figure 1a and is provided in Video S1 (Supporting Information). This clearly illustrates the motion of the graphene flake: initially moving in a straight direction, early alignment with the underlying lattice creates small deflections in the path of the graphene flake, rotating the flake by 60° each time. As the energy of the flake is dissipated in these events, the flake slows down and the alignments create much larger deflections, with the graphene flake center-of-mass motion almost representing a random path. Eventually the flake comes to a stop in a commensurate position.

As we show in Table 1, temperature affects the distance traveled by the flake. Higher temperatures induce a range of frequencies of undulation in the surface (see Figure 2b) which impede a graphene flake from sliding across them. This is illustrated by the kinetic energy of the graphene flake at higher temperatures, which decreases between alignment events due to dissipation of energy to the graphite substrate (see Section VI

in the Supporting Information). The total distance traveled by a flake at higher temperatures is therefore lower. This effect is more pronounced when flakes travel over a suspended graphene sheet, rather than over graphite, since thermally induced undulations are larger in the more flexible substrate, as can be seen in the greater amplitudes in the Fourier transforms of the surface height function given in Figure 2b. Our results indicate that the temperature trend observed in experiment is only a low temperature phenomenon. Between 100 and 200 K we see no change within statistical error in the distances traveled. This is due to a competing effect where the increased internal energy at higher temperatures of the flake and substrate means the flake does not stop as quickly, increasing the distance the flake travels. We tested our system for finite size effects; by doubling the substrate size we show that trends are preserved and numerical values are within error for a larger system (see Section VIII in the Supporting Information).

We also introduced undulations through compressing the substrate. In Figure 2a we observe that compression introduces pronounced long wavelength traveling waves in graphene. Experimentally, suspended graphene is known to produce dynamic ripples^[12] which exhibit similar soliton-like behavior to the waves in our simulation. The simulation was performed at 1 K using a compression of 0.5%, which is within previous experimental compression ranges.^[13] While these waves impede the motion of the flake in the majority of simulations in our ensemble, another transport mechanism dominates in a small number of simulations, where the flake “surfs” in the trough of traveling waves. On compressing a graphene sheet the distance traveled by a flake following propulsion is observed to increase (see Section X in the Supporting Information). For this to occur the flake must be of comparable size to the wavelength of the undulations, and may provide a means of separating graphene flakes by size. A similar mechanism has been observed before in simulation of water droplets on graphene,^[13] but not between 2D materials.

From the above simulations we have characterized three friction and transport mechanisms for superlubric graphene flakes sliding on a graphitic substrate. Alignment events transfer energy between (translational and rotational) kinetic modes within the flake, and between the flake and substrate. This mechanism is temperature independent and is only reliant on lattice matching of substrate and projectile. The second is due to short range undulations caused by thermal fluctuations in the substrate that lead to nonelastic “collisions” with out-of-plane substrate atoms. Finally, we predict that, by compressing the substrate, one can introduce long wavelength undulations that can “carry” a flake, vastly reducing the friction it experiences. Therefore, at temperatures approaching 0 K the only friction a flake could experience would be due to alignment events; raising the temperature would increase the friction experienced. However, long range undulations may actually reduce friction if controlled properly.

To further test the interactions of graphitic systems we simulated various collisions of flakes and different exfoliation scenarios.^[14] Colliding flakes into each other highlights the flexibility of graphene. Given a force of 0.06 kcal mol^{−1} Å^{−1} to each atom in a 10 nm flake for 2.5 ps—which is typical for the sliding simulations above—a flake collides and “bounces off”

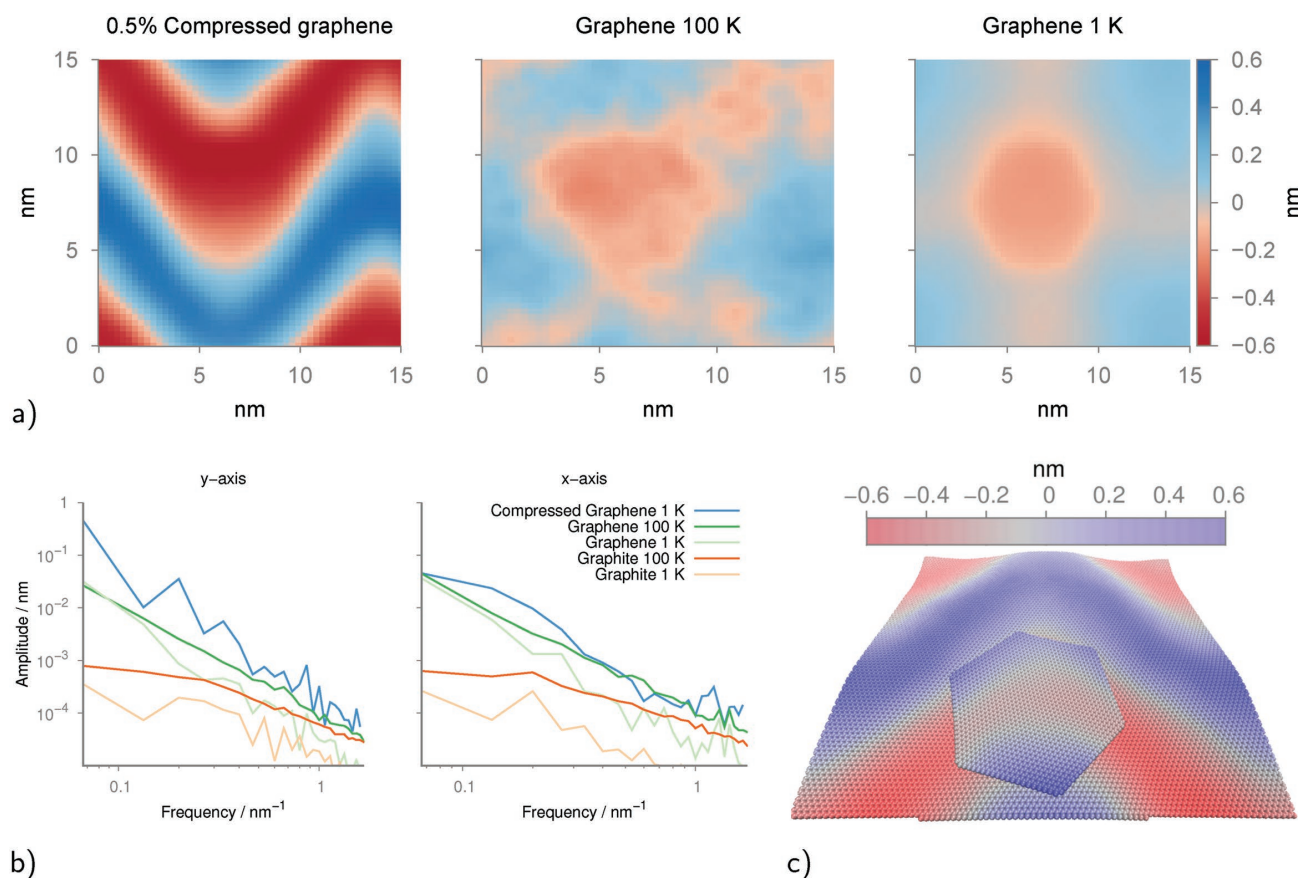


Figure 2. a) Surface roughness for different suspended graphene simulations. Compressing the substrate produces large smooth undulations. Higher temperatures produce random fluctuations. At 1 K there are so few fluctuations that the puckering of the surface due to the graphene flake can be made out. b) Spectral intensity of a 2D Fourier transform of the different surfaces in the x and y directions. The frequencies are averages of all replicas in each ensemble. Graphite is clearly orders of magnitude smoother than the suspended graphene sheets. Vertical axes are identical. c) A graphene flake “surfing” in the trough of a traveling wave made in a compressed suspended graphene sheet. Color represents the height displacement as in (a). Trapped in this trough, it does not align with the surface and so is free to slide without losing energy, see also Video S2 (Supporting Information).

another stationary flake. Given more force the flakes can slide on top of or under one another. The AB stacking of graphite sheets means the flake straddling another flake or a step defect cannot be fully commensurate with both layers; this reduces the contribution of alignment events to the friction experienced; see Section XI in the Supporting Information.

Figure 3 shows different regimes of exfoliating graphene flakes from a graphitic substrate. A harmonic spring, attached to a ring of six carbon atoms at the corner of the graphene flake, was used to induce exfoliation. Perpendicular configurations were used to compare peeling and shearing modes of exfoliation. A peeling mechanism mimics that used by “release tapes,” still the only way to mass produce defect-free single-layer graphene for material purposes.^[15] Using a weighted histogram analysis method^[16] we found that the work done to exfoliate the flake is 40% less via peeling than shearing, contrary to the common belief that a shearing mechanism would be more favorable^[17] (see Section XII in the Supporting Information).

We attribute this difference to the friction that must be overcome when sliding the flake over the substrate. As the flake is sheared it can fall into different commensurate positions; each

time it does so the spring must overcome this barrier to move the flake. Graphene is a flexible 2D material; bending the flake is associated with a lower energy barrier. By peeling the flake, the end still attached to the substrate does not need to leave a commensurate position. When designing exfoliation processes, including surfactants and intercalation agents for graphene liquid phase exfoliation, this peeling mechanism should be targeted.

In summary, GraFF recreates several properties of graphene friction seen experimentally. It elucidates the unusual sliding mechanisms and temperature dependence of graphene in a superlubric state. We show that a full description of friction in graphene systems predicts new behaviors and that exfoliating graphite via peeling is the energetically favored mechanism.

Computational Methods

Simulation Specification: All simulations were carried out using the modeling software LAMMPS.^[18] Simulations used periodic boundary conditions; the timestep was 1 fs; Coulombic interactions were calculated using a particle–particle particle–mesh with a precision of $0.0001 \text{ kcal mol}^{-1} \text{ \AA}^{-1}$; the cut-off for Lennard–Jones interactions

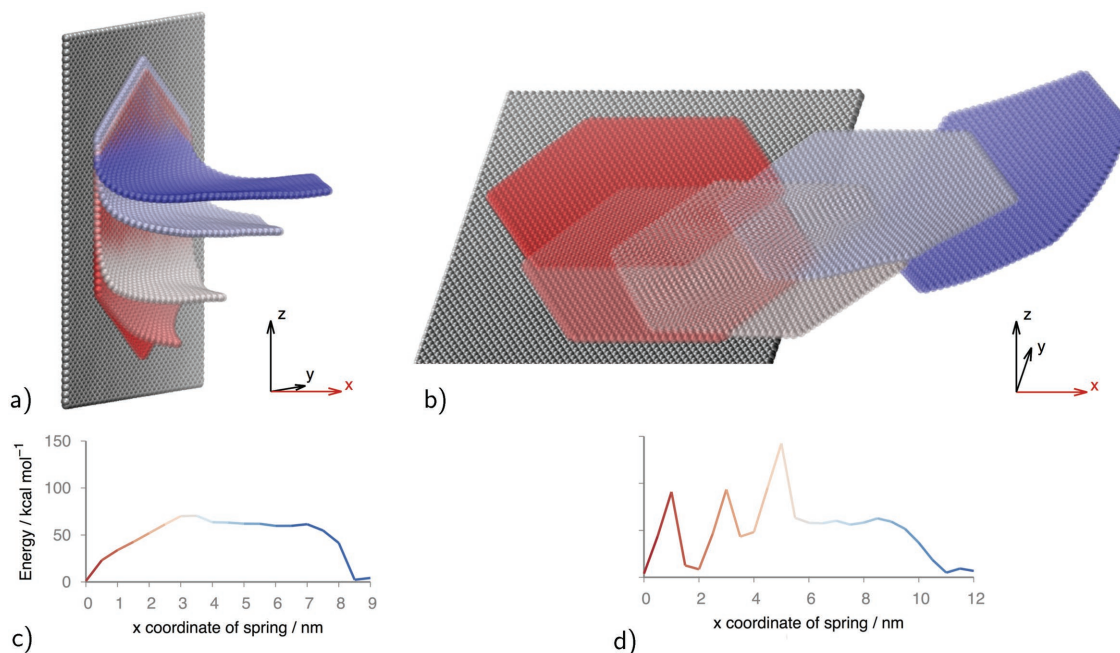


Figure 3. Steered simulations of two exfoliation mechanisms. 10 nm graphene flakes are pulled by a corner from a graphitic substrate with a harmonic spring along the x axis. The spring was allowed to move in the y and z planes; the energy in the spring per atom is shown in plots (c) and (d). (a) and (c) exhibit a peeling mechanism. (b) and (d) manifest a shearing mechanism. Spikes in the spring's energy are due to the flake becoming trapped in commensurate positions with the substrate.

was 11 Å; bonds, angles, dihedrals, and impropers were implemented as specified by the OPLS forcefield; CH intermolecular interactions were unchanged from the OPLS definition, only the graphene carbon intermolecular interactions were changed with GraFF (see below and Section I in the Supporting Information).

Minimizations used a conjugate gradient method with a force tolerance of 1×10^{-6} kcal mol⁻¹ Å⁻¹ and energy tolerance of 1×10^{-6} kcal mol⁻¹.

Canonical (NVT) and isothermal–isobaric (NPT) ensemble simulations used a Nosé–Hoover barostat and thermostat.

Simulation Setup: Starting configurations were generated using crystallographic measurements for graphite: carbon bond lengths of 1.42 Å and interlayer spacing of 3.35 Å.^[19] Graphene flakes were terminated with hydrogen atoms and were laterally 10 nm at their widest point, containing 2520 atoms. Graphite substrates were simulated with four graphene sheets stacked in an ABAB arrangement, with a flat 12-6 Lennard–Jones potential acting as a wall at the bottom of the simulation. The wall potential was matched to that of graphite in OPLS $\epsilon = 0.07$ kcal mol⁻¹; $\sigma = 3.4872$ Å. Simulation dimensions with graphite substrates were 15 nm × 15 nm × 3.5 nm; simulations with graphene substrates were 15 nm × 15 nm × 2.5 nm, giving a vacuum spacing of at least 15 Å.

These structures were energy minimized within LAMMPS, with subsequent initial velocities generated from a Maxwell–Boltzmann distribution and equilibrated in the NPT ensemble for 500 ps at the required temperature. All simulations contained a graphitic substrate extending throughout the xy plane, with a vacuum space in the z direction; therefore the pressure was only equilibrated in the x and y directions.

Compression studies used a 20 nm × 20 nm graphene sheet, while coordinates were scaled by the compression factor before equilibration in the NVT ensemble.

Propulsion of the flakes was simulated by applying a constant 0.06 kcal mol⁻¹ Å⁻¹ to each atom in the flake. This was determined to be the smallest force, within 0.01 kcal mol⁻¹ Å⁻¹, required to push the flake out of its commensurate position. The force was applied to the flake until it had moved 2 Å from its starting position, which took an average of 2.5 ps, after which no further force was added to the atoms (2 Å was

the distance an STM tip was in contact with the flake in experiment^[1]). The distance traveled was measured relative to an atom in the underlying substrate to remove the effects of drift from results.

Rotational energy was calculated by defining an orientational vector between two atoms in the flake and measuring the angle rotated every 5 ps interval.

After equilibration, propulsion and subsequent sliding were simulated in the micro-canonical (NVE) ensemble. This ensemble was chosen as adding force to the atoms in the flake injects energy into the system which a thermostat would immediately try to remove by altering the velocities. The NVE ensemble preserves this uneven energy distribution so we can observe how the flake dissipates its energy to the substrate.

The steered exfoliation simulations used similarly equilibrated systems in the NVT ensemble. The substrate was fixed so the substrate did not move with the spring. The substrate was a 15 nm × 15 nm graphene sheet. The peeling exfoliation had a simulation box of 15 nm × 15 nm × 12 nm; the shearing exfoliation had a simulation box of 22 nm × 15 nm × 2 nm (see Figure 3), corresponding to a 12 nm vacuum space. The spring was attached to the six carbon atoms in a ring at the corner of the flake and had a spring constant of 5 kcal mol⁻¹. The spring was moved 1 Å every 100 ps along the exfoliation pathway and allowed to move freely in the other directions. This results in an effective pulling speed of 1 m s⁻¹. The averages for each position were taken over the last 50 ps at each point. Free energies were calculated using a weighted histogram analysis method.^[16]

A New Forcefield for Graphene and Graphite: GraFF was developed to address problems with existing simple Lennard–Jones potentials in representing graphene–graphene interactions. The common forcefields tested either overestimate the absorption energy of graphite or underestimate the energy barrier to sheets sliding past each other (see Tables 2 and 3).

Tables 2 and 3 show the results of simulations testing the adsorption and friction, respectively, of graphene using different forcefields. Energies are derived from static calculations: sliding a graphene sheet over another (Table 2), and removing the top layer of a graphite stack (Table 3). See Section I in the Supporting Information for further details of these calculations.

Table 2. Results of a simulation where two sheets of graphene slide past each other using various established forcefields.

Method	Energy barrier [meV]
DFA+MBD ^[20]	1.58
GAFF ^[21]	1.35
OPLS ^[22]	0.34
Dreiding ^[23]	0.34
COMPASS ^[24]	0.06
GraFF	1.15

Using the OPLS forcefield^[26] as a basis, an angular term was added to the nonbonded interaction energies. To achieve this two carbon atoms were taken in different graphene layers, C_1 and C_2 , and a reference carbon atom, C_R , bonded to C_1 . The parameters are then: θ_{R12} , the angle made by $C_R C_1 C_2$; and $r_{C,C}$, the distance between C_1 and C_2 . Then a 12-6 Lennard–Jones potential was weighted by a $\cos^2(2\theta_{R12})$ term, so that the energy was at a minimum at 90° and was brought smoothly to zero at 45° . This also made the angular dependence of the carbon atom potentials resemble a p-orbital in the regions above and below the graphene sheet where electron overlap can occur. Note that C_R is a reference atom, and is merely used to define the orientation, but was not included in the potential energy. Therefore:

$$V_{\text{GraFF}}(r_{C_1 C_2}, \theta) = \begin{cases} 0, & 0^\circ < \theta < 45^\circ \\ V_{\text{LJ}}^{12-6}(r_{C_1 C_2}) \cdot \cos^2(2\theta), & 45^\circ < \theta < 135^\circ \\ 0, & 135^\circ < \theta < 180^\circ \end{cases} \quad (1)$$

where:

$$V_{\text{LJ}}^{12-6}(r) = 4\epsilon \left[\left(\frac{\sigma}{r} \right)^{12} - \left(\frac{\sigma}{r} \right)^6 \right] \quad (2)$$

In the original OPLS forcefield $\epsilon_{\text{OPLS}} = 0.07$ kcal mol⁻¹ and $\sigma_{\text{OPLS}} = 3.55$ Å. Charges were ± 0.115 for terminating hydrogens and carbons, respectively. For GraFF a standard Lennard–Jones potential was combined where $\epsilon_{\text{LJ}} = 0.02$ kcal mol⁻¹ and $\sigma_{\text{LJ}} = 3.55$ Å with the

Table 3. Adsorption energy of the upper sheet of a graphite stack using various forcefields.

Method	Adsorption energy [meV per atom]
Experiment	
Zacharia et al. ^[2]	61 ± 5
Liu et al. ^[3]	31 ± 2
Benedict et al. ^[4]	35 +15/–10
Experimental range	25–66
DFT	
vdw-DF2 ^[5]	50.8
vdw-optPBE ^[5]	61.7
LAMMPS simulations	
GAFF ^[21]	99.9
OPLS ^[22]	54.5
Dreiding ^[23]	81.3
COMPASS ^[24]	61.0
GraFF	56.8

weighted angular potential where $\epsilon_{\text{Angular}} = 0.025$ kcal mol⁻¹ and $\sigma_{\text{Angular}} = 3.627$ Å; charges were unchanged. These parameters were chosen by recursive improvement of the adsorption energy and sliding potential, summarized in Tables 2 and 3. Increasing the weighting factor of GraFF increased the barrier to sliding while increasing the weighting of the ordinary Lennard–Jones parameter increased the adsorption energy.

Ensembles and Averages: These types of simulation are extremely sensitive to their starting configuration. To report reproducible results, a large ensemble of 180 replicas was undertaken to characterize the system's global behavior.^[25] Each replica started with unique, uncorrelated atomic velocities drawn from a Maxwell–Boltzmann distribution but were otherwise identical. The straight-line distance traveled by the flake after propulsion was used as the characteristic quantity to study as this was the only information experimentally accessible. These distances fit a log-normal distribution (see Section IV in the Supporting Information), which is typical for many natural processes.^[26] A bootstrap with replacement was performed on this sample to quantify the confidence in the results that were derived. A “resample” from the original 180 simulations was taken, at random with replacement, of size N . This was done 10 000 times and the standard error from the distribution of averages from all resamples gave the confidence interval. It was deemed that the point of diminishing return arrived at about $N = 40$ (see Section IV in the Supporting Information). Quantities used in Table 1 were derived from ensembles of 40 replicas; errors were given as the confidence interval of one standard deviation, derived from a separate bootstrap on that ensemble with a resample size of 40.

Supporting Information

Supporting Information is available from the Wiley Online Library or from the author.

Acknowledgements

The authors thank the Engineering and Physical Sciences Research Council (EPSRC) for a studentship for R.C.S. and acknowledge partial funding from the EU H2020 Research Innovation programme for the ComPat project <http://www.compat-project.eu/> under grant agreement no. 671564. Simulations were run on ARCHER at Edinburgh Parallel Computing Centre www.archer.ac.uk, on SuperMUC at Leibniz Supercomputing Centre (LRZ) www.lrz.de and on Prometheus at Cyfronet <http://www.cyfronet.krakow.pl/>. Supercomputing time on ARCHER was provided by the UK Consortium on Mesoscale Engineering Sciences (UKCOMES) under the UK EPSRC Grant No. EP/L00030X/1; access to SuperMUC and Prometheus came from supercomputing awards at LRZ and Cyfronet. R.C.S., J.L.S., and P.V.C. conceived and designed the project. R.C.S. performed the molecular dynamics simulations and subsequent analysis. All the authors contributed to discussions and wrote the paper.

Conflict of Interest

The authors declare no conflict of interest.

Keywords

2D-materials exfoliation, atomistic simulations, graphene, superlubricity

Received: October 5, 2017

Revised: November 28, 2017

Published online: February 13, 2018

- [1] X. Feng, S. Kwon, J. Y. Park, M. Salmeron, *ACS Nano* **2013**, *7*, 1718.
- [2] R. Zacharia, H. Ulbricht, T. Hertel, *Phys. Rev. B* **2004**, *69*, 155406.
- [3] Z. Liu, J. Z. Liu, Y. Cheng, Z. Li, L. Wang, Q. Zheng, *Phys. Rev. B* **2012**, *85*, 205418.
- [4] L. X. Benedict, N. G. Chopra, M. L. Cohen, A. Zettl, S. G. Louie, V. H. Crespi, *Chem. Phys. Lett.* **1998**, *286*, 490.
- [5] Z. Wang, S. M. Selbach, T. Grande, *RSC Adv.* **2014**, *4*, 3973.
- [6] M. Dienwiebel, G. S. Verhoeven, N. Pradeep, J. W. M. Frenken, J. A. Heimberg, H. W. Zandbergen, *Phys. Rev. Lett.* **2004**, *92*, 126101.
- [7] R. Guerra, U. Tartaglino, A. Vanossi, E. Tosatti, *Nat. Mater.* **2010**, *9*, 634.
- [8] E. Koren, E. Lörtscher, C. Rawlings, A. W. Knoll, U. Duerig, *Science* **2015**, *348*, 679.
- [9] M. Pykal, P. Jurečka, F. Karlický, M. Otyepka, *Phys. Chem. Chem. Phys.* **2015**, *18*, 6351.
- [10] C.-J. Shih, S. Lin, M. S. Strano, D. Blankschtein, *J. Am. Chem. Soc.* **2010**, *132*, 14638.
- [11] I. V. Lebedeva, A. A. Knizhnik, A. M. Popov, O. V. Ershova, Y. E. Lozovik, B. V. Potapkin, *Phys. Rev. B* **2010**, *82*, 155460.
- [12] J. C. Meyer, A. K. Geim, M. I. Katsnelson, K. S. Novoselov, T. J. Booth, S. Roth, *Nature* **2007**, *446*, 60.
- [13] M. Ma, G. Tocci, A. Michaelides, G. Aeppli, *Nat. Mater.* **2016**, *15*, 66.
- [14] M. Cai, D. Thorpe, D. H. Adamson, H. C. Schniepp, *J. Mater. Chem.* **2012**, *22*, 24992.
- [15] S. J. Kim, T. Choi, B. Lee, S. Lee, K. Choi, J. B. Park, J. M. Yoo, Y. S. Choi, J. Ryu, P. Kim, J. Hone, B. H. Hong, *Nano Lett.* **2015**, *15*, 3236.
- [16] A. Grossfield, WHAM: the weighted histogram analysis method, <http://membrane.urmc.rochester.edu/content/wham> (accessed: June 2017).
- [17] C. Fu, X. Yang, *Carbon* **2013**, *55*, 350.
- [18] S. Plimpton, *J. Comput. Phys.* **1995**, *117*, 1.
- [19] P. Delhaes, *Graphite and Precursors*, Gordon and Breach Science Publishers, Amsterdam, The Netherlands **2001**.
- [20] W. Gao, A. Tkatchenko, *Phys. Rev. Lett.* **2015**, *114*, 096101.
- [21] D. Case, R. Betz, W. Botello-Smith, D. Cerutti, T. Cheatham III, T. Darden, R. Duke, T. Giese, H. Gohlke, A. Goetz, N. Homeyer, S. Izadi, P. Janowski, J. Kaus, A. Kovalenko, T. Lee, S. LeGrand, P. Li, C. Lin, T. Luchko, R. Luo, B. Madej, D. Mermelstein, K. Merz, G. Monard, H. Nguyen, H. Nguyen, I. Omelyan, A. Onufriev, D. Roe, A. Roitberg, C. Sagui, C. Simmerling, J. Swails, R. Walker, J. Wang, R. Wolf, X. Wu, L. Xiao, D. York, P. Kollman, *AMBER 2016*, University of California, San Francisco, CA **2016**.
- [22] W. L. Jorgensen, D. S. Maxwell, J. Tirado-Rives, *J. Am. Chem. Soc.* **1996**, *118*, 11225.
- [23] E. N. Skountzos, A. Anastassiou, V. G. Mavrantzas, D. N. Theodorou, *Macromolecules* **2014**, *47*, 8072.
- [24] H. Sun, *J. Phys. Chem. B* **1998**, *102*, 7338.
- [25] P. V. Coveney, S. Wan, *Phys. Chem. Chem. Phys.* **2016**, *18*, 30236.
- [26] J. Gaddum, *Nature* **1945**, *156*, 463.